Characterization and Application of Nanomaterials (2023) Volume 6 Issue 1
doi:10.24294/can.v6i1.3406

ORIGINAL RESEARCH ARTICLE

Morphology, structural and thermal degradable properties of carboxymethyl cellulose/Cuo nanoparticles for tetracycline removal in model aqueous solution

Win Pa Pa Phyo[1], Yamin Thet[1,2], May Thazin Kyaw[1], Ngwe Sin[1], Aung Than Htwe[1,3*]

[1]*Department of Chemistry, University of Yangon, Kamaryut 11041, Yangon, Myanmar. E-mail: aungthanhtwe76@gmail.com*

[2] *Department of Chemistry, Bamaw University, Bamaw 01132, Kachin State, Myanmar.*

[3] *Department of Chemistry, Mohnyin University, Mohnyin 01162, Kachin State, Myanmar.*

ABSTRACT

Broad-spectrum antibiotics, such as tetracyclines, are used to treat and manage a range of infectious disorders. Since the kidneys are the primary organs responsible for excreting tetracyclines, clinicians should refrain from prescribing them to patients who have renal failure. Tetracyclines are one of the clinical waste products of today. One of the biggest problems in the field of pollution of the environment today is the persistence of different pharmaceutical residues, drug residues, pesticides, and metal ion species of the new-generation pollutants in surfaces and groundwater. In the present work, carboxymethyl cellulose (CMC)-CuO nanoparticles (CMC-CuO NPs) were synthesized using CuO NPs within different amounts of CMC (0.5, 1.0, 1.5 and 2.0 g) at 85 °C. The synthesized nanoparticles were characterized by XRD, FT IR, SEM, and TG-DTA analysis. According to XRD and SEM, the crystallize size and morphology influenced the dosage of CMC. FT-IR analysis confines the layer of CMC to the CuO nanoparticle surface. TG-DTA results indicated that the CMC content of CMC-CuO NPs was between the range of 69% and 75% by weight. The effects of some parameters such as initial concentration, pH, adsorbent dosage, and contact time on the adsorption of tetracycline from aqueous model solutions on CMC-CuO NPs were investigated with batch studies. It was found that the removal of tetracycline was obtained about 80% with optimized parameters of 10 mg/L concentration, 180 min contact time, 5 pH, and 0.3 g/25 mL dose. The synthesized CMC-CuO NPs nanocomposite may be a promising material for the removal of tetracycline in environmental pollution and toxicology.

Keywords: Carboxymethyl Cellulose; CuO NPs; Morphology; Removal of Tetracycline

ARTICLE INFO

Received: 9 April 2023
Accepted: 22 May 2023
Available online: 4 June 2023

1. Introduction

They are discharged into water sources and domestic wastewater by some pharmaceutical companies. Due to their widespread use worldwide, antibiotics are among the pharmaceutical products and drug residues of greatest concern. This is due to the harmful effects of antibiotics on the hepatocytes and other organs of gastrointestinal organs. Many microorganisms, including beneficial bacteria such as proteobacteria, cyanobacteria, algae, bacteria, and ammonium-oxidizing bacteria, are harmful to antibiotics in water. An antibiotic called tetracycline is commonly used to treat various diseases in humans. This is the second-most-used antibiotic in the world. Tetracycline also inhibits nitrification, soil microbial respiration, and iron(III) reduction[1]. In view of these facts, several adsorption techniques have been reported to remove tetracycline antibiotics from water[2–5]. The nanocomposite material is

made from a polymer-coated substrate that functions as a hybrid adsorbent to remove pollutants. The mixture widely used in environmental cleaning is formed by polycations that attach to carboxymethylcellulose, which carries a negative charge. These synthetic materials are used to remove organic pollutants such as heavy metals, antibiotics, organic dyes, and pesticides. On the other hand, neither polyanion adsorption on positively charged minerals nor microbial respiration in soil have been reported as new synthetic materials for antibiotic removal[1]. These results led to the publication of several adsorption techniques to remove tetracycline antibiotics from water[6].

As a linear polymer with high molecular weight, high crystallinity, and strong intramolecular hydrogen bonds, cellulose is organic, renewable, and biodegradable. Most organic solvents cannot dissolve it[7,8]. One way to improve the efficiency of cellulose is to convert it into derivatives such as carboxymethyl cellulose (CMC), based on the ether reaction of B. Williamson[9,10]. The long-chain, anionic, and water-soluble properties of CMC make it important. Due to its low cost, low toxicity, ability to form transparent films, high viscosity, biodegradability, and biocompatibility, CMC is considered a substitute for synthetic polymers[11]. The abundance of hydroxyl (-OH) and carboxyl (-COOH) groups in carboxymethyl cellulose (CMC) increases its hygroscopicity. Copper oxide (CuO) is widely used in many fields, including catalysts, ceramics, glass, and antibacterial agents. The production of CuO NPs is inexpensive compared to gold and silver nanoparticles. In addition, CuO NPs also have excellent and strong antibacterial activity, and appreciation for their unique crystal structure. When it comes to how the nanoparticles ultimately interact with target cells, their size, state of aggregation in liquids, and surface charge are among their physical and chemical characteristics that matter[12].

In the current work, the specific objective of the present study was to synthesize carboxymethyl cellulose/CuO nanoparticles (CMC-CuO NPs), involving the co-precipitation of CMC polymer network in the presence of CuO NPs, to characterize the CMC-CuO NPs nanoparticles synthesized by modern technique as XRD, FT IR, SEM, and TG-DTA, and to evaluate synthesized CMC-CuO NPs as adsorbents to remove tetracycline from model aqueous solution.

2. Materials and methodology

2.1 Materials

Sodium carboxymethyl cellulose (CMC) with a degree of substitution (DS) 0.55–1.0 and a viscosity of 15,000 mPa/s (1% in H_2O, 25 °C) was obtained from Nippon Paper Chemicals Co., Ltd., Japan. Other chemicals such as epichlorohydrin (99.5%), copper(II) sulphate pentahydrate ($CuSO_4 \cdot 5H_2O$), sodium hydroxide (NaOH), acetic acid glacial (CH_3COOH, 100% (v/v)) and hydrochloric acid (HCl) were purchased from Merck (Indonesia).

2.2 Preparation of the CuO nanoparticles

The copper(II) oxide nanoparticles (CuO NPs) were prepared by co-precipitation method. Firstly $CuSO_4 \cdot 5H_2O$ was dissolved in 100 mL distilled water and stirred continuously. Sodium hydroxide (5 M) was added dropwise into the mixture until the solution reached pH 12 and stirred continuously for 6 h at 85 °C. The black precipitation was obtained and washed several times with distilled water to remove any alkali metals until a neutral state (pH 7). And then, this was washed again with ethanol 5 times. Samples were dried in a hot air oven at 80 °C for 16 h. The sample was calcined at 500 °C for 4 h and crushed in mortar and pestle. Finally, the sample in the crucible was allowed to cool at room temperature.

2.3 Preparation of carboxymethyl cellulose/CuO nanoparticles

A total of 1.0 g of copper oxide nanoparticles was mixed with epichlorohydrin (2.5 mL) and 25% acetic acid (30.0 mL). The mixture was stirred for 12 h on a magnetic stirrer to obtain the CuO NPs mixture solution. The different amounts of 0.5, 1.0, 1.5, and 2.0 g of CMC sample were added to the CuO NP mixture solution and then stirred for 30 min. This was endorsed to stand for 24 h. Finally, CuCMC was dried for 12 h at 60 ºC and collected. The obtained samples are coded as 0.5CMC-CuO NPs for 0.5 g of CMC, 1.0CMC-CuO NPs for 1.0 g

of CMC, 1.5CMC-CuO NPs for 1.5 g of CMC, and 2.0CMC-CuO NPs for 2.0 g of CMC.

2.4 Characterization and analysis

X-ray characterization of the synthesized products was performed by X-ray diffractometer at room temperature using Cu Kα radiation (λ = 1.5406 °A) with the 2θ range 5–80°. The crystallite size of the CMC-CuO NPs was evaluated from X-ray analysis data using a modified Debye-Scherrer Equation. The chemical groups involved in synthesized CMC-CuO NPs were identified using the Fourier transform infrared spectroscope (FTIR Perkin-Elmer, RX1) method. The size, and morphology of the synthesized product of CMC-CuO NPs were determined by scanning electron microscopy (SEM). TGA and DTA were performed with a TG Setaram instrument (France) in the air of argon (30 to 600 °C).

2.5 Adsorption studies

Adsorption by the batch technique was used to study TC removal using CuO NPs and CMC-CuO NPs. First, the accurate TC amount was dissolved in methanol and deionized water to make stock solutions of TC at a concentration of 100 mg/L. Then, the stock solutions were taken for dilution to make a daily solution. At 25 °C, different adsorbent volumes were mixed with 25 mL of TC solution in 100 mL Erlenmeyer flasks. The concentration of the solution, contact time, pH of the solution, and adsorbent dose are a few important parameters that affect the removal of TC. All concentrations of TCs in aqueous solutions were analyzed by the ultraviolet-visible (UV-Vis) method at 277.4 nm using a GENESYS 10S (Thermo Scientific) UV-Vis spectrometer.

$$\text{removal efficiency (\%)} = \frac{C_i - C_f}{C_i} \times 100\ \% \qquad (1)$$

where C_i and C_f are the initial and final concentrations of TC (mg/L).

3. Results and discussion

3.1 Characterization of CuO NPs and CMC/CuO NPs

3.1.1 XRD analysis

The XRD pattern of the CuO NPs and CMC/CuO NPs in the 2θ range of 20–80θ is shown in **Figure 1**. The diffractogram of the CMC/CuO NPs is assigned to diffractions at 2θ values of about 32°, 35°, 38°, 48°, 53°, 58°, 61°, 65°, 66°, 72°, and 75°, which assigned to the (110), (–111), (111), (–202), (020), (202), (–113), (–311), (220), (311) and (044) diffractions of CuO NPs, respectively[13]. All the peaks match well with those of monoclinic-phase CuO NPs and confirm the formation of CMC-CuO NPs matrix. No impurity peaks were observed in the XRD patterns, indicating the high purity of the obtained CuO particles. A wide peak at 24° is due to the polymer networks. Briefly, the XRD results confirmed the crystallinity of the prepared CMC/CuO NPs with the presence of CuO[1,14]. Using Scherrer's equation, the calculated average crystallite size of the CuO NPs, 0.5CMC-CuO, 1.0CMC-CuO, 1.5CMC-CuO and 2CMC-CuO were found as 21.22, 38.16, 50.07, 59.99 and 61.28 nm, respectively. There was no change in the crystal structure, which showed diffraction peaks at the same 2θ position in all diffractograms. However, the crystallite size changed. Furthermore, crystallite size increased with the increasing amount of CMC. The higher the CMC content, the higher the crystallite size of CMC-CuO NPs produced.

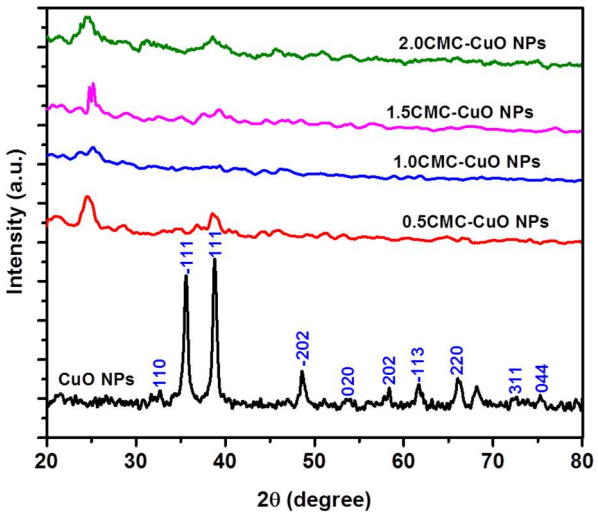

Figure 1. XRD patterns of the CuO NPs and CMC-CuO NPs.

3.1.2 SEM analysis

SEM images of the CuO NPs and CMC-CuO NPs are shown in **Figure 2**. In **Figure 2**, a clear and uniform surface morphology was observed for the CuO NPs. However, there are visible spherical par-

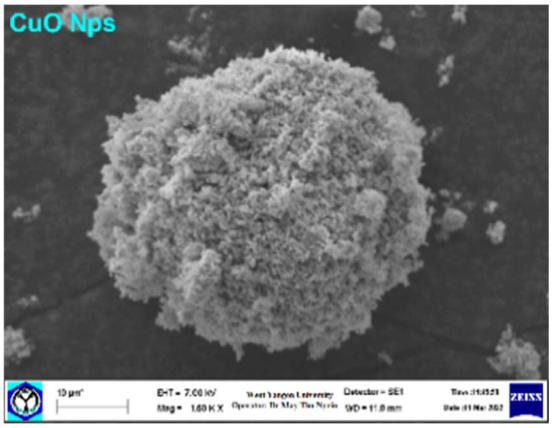

(a) CuO NPs

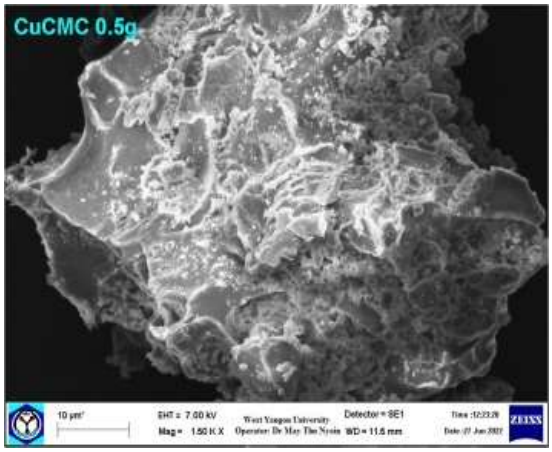

(b) 0.5CMC-CuO NPs

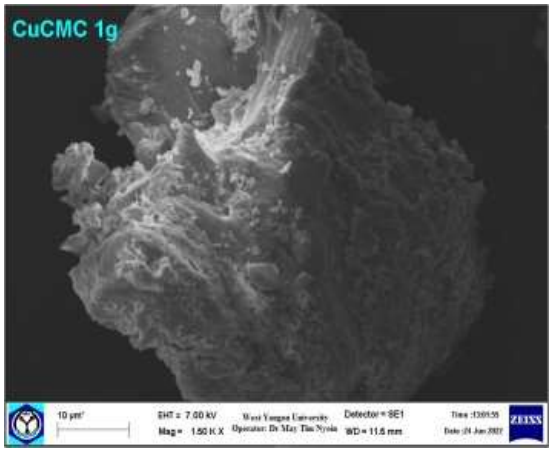

(c) 1.0CMC-CuO NPs

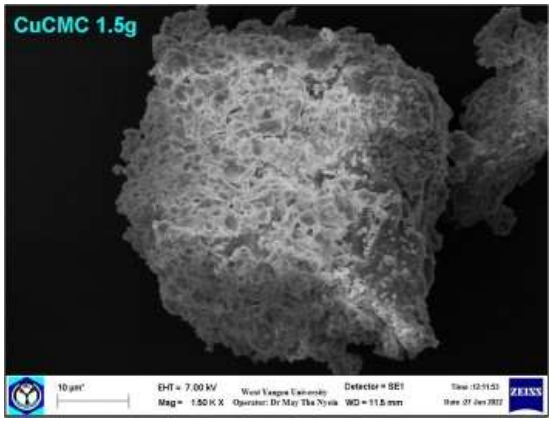

(d) 1.5CMC-CuO NPs

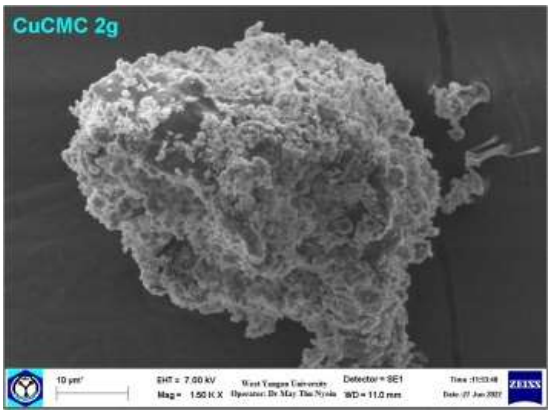

(e) 2.0CMC-CuO NPs

Figure 2. SEM images of the CuO NPs and CMC-CuO NPs.

ticles in the case of nanoparticles containing CMC (**Figure 2(b)** to **(e)**). SEM results showed that the CMC matrix was dispersed in the CuO NPs solution. However, **Figure 2(e)** found that some aggregation and bigger particles can be seen for CMC-CuO NPs containing increasing CMC content.

3.1.3 FTIR analysis

The functional groups present in CuO NPs and CMC-CuO NPs were studied by Fourier Transform Infrared (FTIR) spectroscopy. The FTIR spectra of CuO NPs and CMC-CuO NPs were recorded in the range of 4,000–400 cm^{-1} using KBr pellet technique Perkin Elmer spectrometer. The FT IR spectra of CuO NPs and CMC-CuO NPs are shown in **Figures 3(A)** and **(B)**. The broad absorption bands that appeared at 3,469–3,272 cm^{-1} were due to OH stretching of the alcoholic OH group while OH bending appeared at 1,356 cm^{-1}. The band at 2,993 cm^{-1} and 2,867 cm^{-1} showed asymmetric and symmetric C-H stretching vibration of CH_2 groups and their C-H bending vibration occurred at 1,442 cm^{-1}. The bands at 1,735 cm^{-1} and 1,649 cm^{-1} showed the stretching vibration of α, β–unsaturated carbonyl groups. The absorption bands at 1,263 cm^{-1} and 1,052 cm^{-1} appeared by stretching vibration of cyclic ether groups[15]. Additionally, the peaks at 626–687 cm^{-1} can be attributed to the Cu-O vibration of copper oxide nanoparticles. This result corroborated that CMC-CuO could be synthesized.

3.1.4 TG-DTA analysis

The thermal properties of CuO NPs and CMC-CuO NPs were investigated by analytical techniques of TG-DTA. **Figure 4(A)** shows that the

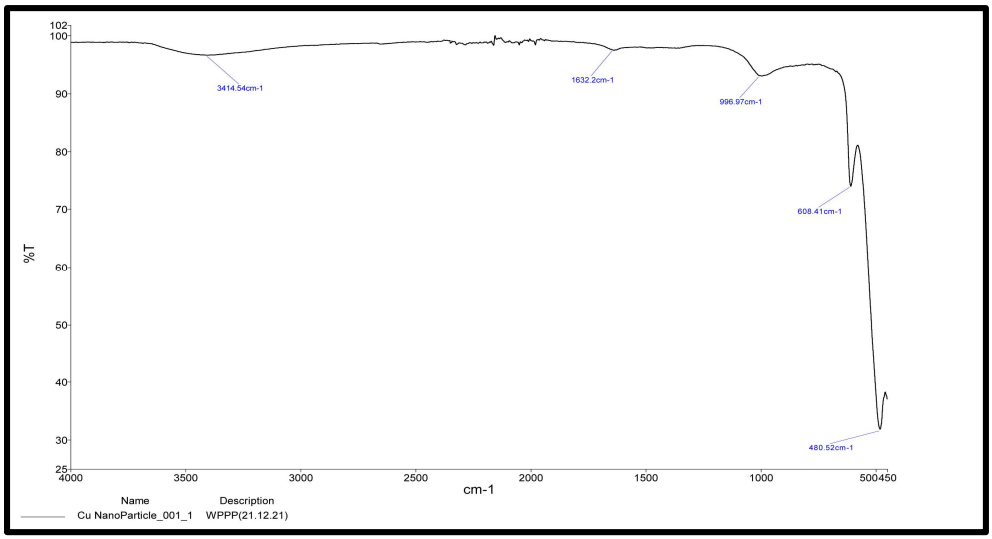

(A)

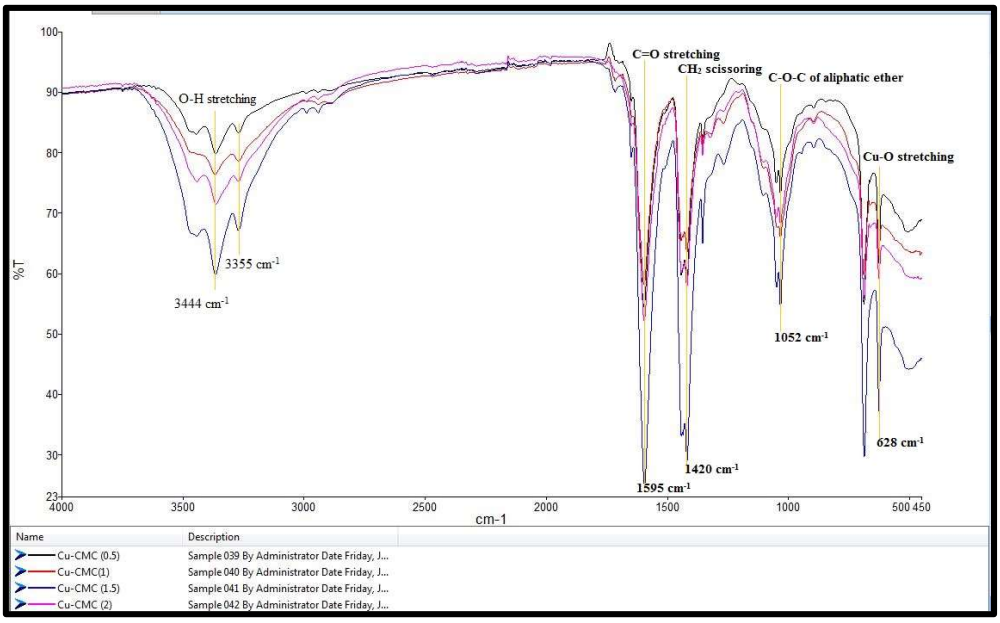

(B)

Figure 3. FT IR spectra of **(A)** CuO NPs and **(B)** CMC-CuO NPs.

CuO NPs have a total weight loss of 4.8% in the range of 37 °C to 243 °C. This is due to the evaporation of water or OH groups adsorbed on the surface of the CuO. According to the CuCMC-CuO NPs curves in **Figure 4(A)**, the temperature range between 37 °C and 280 °C lost 43.50% for 0.5CuCMC-CuO NPs, 42.05% for 1.0CuCMC-CuO NPs, 44.92% for 1.5CuCMC-CuO NPs, and 57.66% for 2.0CuCMC-CuO NPs, corresponding to exothermic peaks at 265 °C [0.5CuCMC-CuO NPs in **Figure 4(B)**], 230 °C [1.0CuCMC-CuO NPs in **Figure 4(B)**], 237 °C [1.5CuCMC-CuO NPs in **Figure 4(B)**], and 243 °C [2.0CuCMC-CuO NPs in **Figure 4(B)**]. This is due to the dehydration process of moisture on CMC-CuO NPs. The loss in weight of 31.22% for 0.5CuCMC-CuO NPs, 35.06% for 1.0CuCMC-CuO NPs, 29.54% for 1.5CuCMC-CuO NPs, and 10.8% for 2.0CuCMC-CuO NPs were observed to take place within the temperature range of 281 °C to 480 °C. **Figure 4(B)** shows sharp broad exothermic peaks at 342 °C (0.5CuCMC-CuO NPs), 324 °C (1.0CuCMC-CuO NPs), 334 °C (1.5CuCMC-CuO NPs), and 330 °C (2.0CuCMC-CuO NPs). This is due to the decomposition of the substituted sites in the methylated derivatives. As a result, aside from depolymerization and pyrolysis, the main polymer chain weight loss was caused by CMC decomposition on the

CuO NPs. It was also confirmed that the CuO NPs were successfully dispersed by CMC.

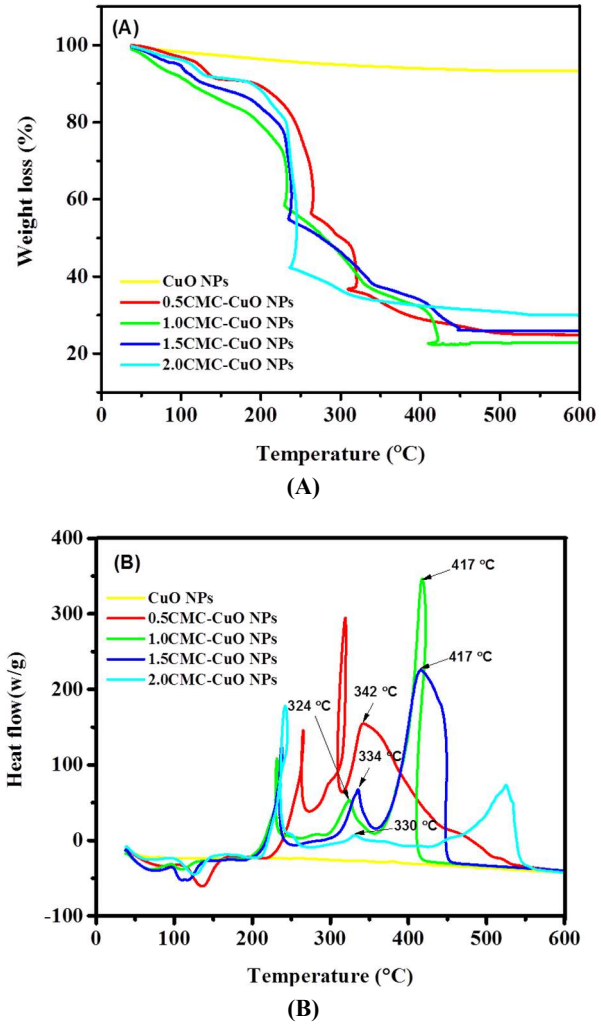

Figure 4. (A) TGA curves and **(B)** DTA curves for CuO NPs and CMC-CuO NPs.

3.2 Investigation of the removal percent of tetracycline (TC)

3.2.1 Effect of initial concentration of TC

Different initial TC concentrations in CuO NPs, and CMC-CuO NPs are shown in **Figure 5**. TC adsorption percentage at different TC concentrations ranging from 10 mg L^{-1} (ppm) to 50 mg L^{-1} (ppm). **Figure 5** shows that when TC concentration increased, TC removal decreased because there were few active sites on the surface of the sorbent. As the data clearly show that removal percent of TC by CMC-dispersed CuO nanoparticles (0.5CMC-CuO NPs (60.12%), 1.5CMC-CuO NPs (61.22%), 1.5CMC-CuO NPs (63.31%), and 2.0CMC-CuO NPs (63.63%)) was considerably higher than that of CuO NPs (42.12%). Therefore, the optimum initial concentration of 10 ppm of TC was chosen for further studies.

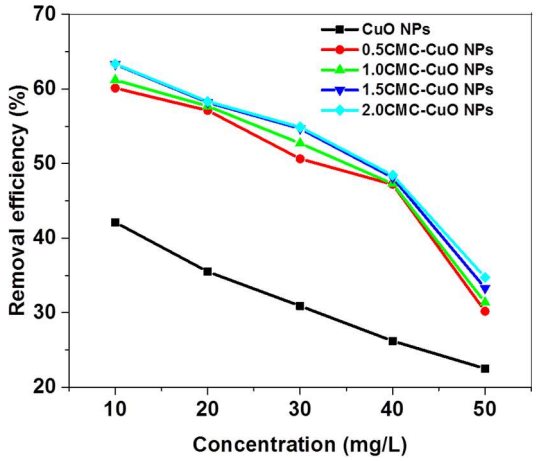

Figure 5. Effect of initial concentration on the TC removal using CuO NPs and CMC-CuO NPs.

3.2.2 Effect of pH

The effect of pH on the TC removal using CuO NPs and CMC-CuO NPs is shown in **Figure 6**. The experiment on the pH effect was conducted in the pH range of 3–9 to find out the best pH for TC removal using CuO NPs and CMC-CuO NPs. **Figure 6** shows that the TC removal using CuO NPs and CMC-CuO NPs reached the maximum at pH 5 and then decreased from pH 6 to 9. As the data clearly show that the removal percent of TC by CMC-dispersed CuO nanoparticles (0.5CMC-CuO NPs (67.85%), 1.0CMC-CuO NPs (70.39%), 1.5CMC-CuO NPs (72.19%), and 2.0CMC-CuO NPs (80.20%)) was considerably higher than that of CuO NPs (50.39%) at pH 5. TC has three different pKa values: 3.3, 7.7, and 9.7. As a result, in aqueous solutions, TC can be found in the cation, zwitterion, or anion form in the pH range 3.3–7.7 below pH 3.3 and in the pH range 3–9 above pH 7.7[16]. At pH 4, the negative charge surface of CMC is convenient for attaching the cationic and zwitter ionic species of TC. This result is similar to the previous report by Parolo *et al.*[17]. Because the negative percentage of the TC zwitterionic form grew as the pH rose from 6 to 8, TC removal was reduced. On the other hand, we found less adsorption at pH > 8 because of stronger electrical repulsion between the negatively charged CMC surface and the anionic TC. As a result, pH 5 is chosen and maintained for

TC removal using CMC-CuO NPs.

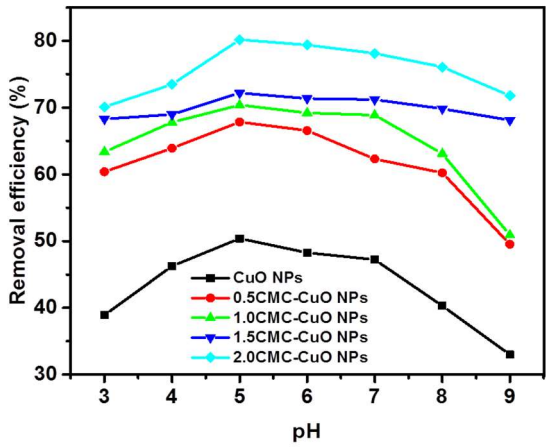

Figure 6. Effect of pH on the TC removal using CuO NPs and CMC-CuO NPs (C_i = 10 mg/L).

3.2.3 Effect of contact time

The influence of contact time on TC removal using CuO NPs and CMC-CuO NPs is shown in **Figure 7**. The contact time increased from 30 to 240 min. **Figure 7** indicates that TC removal using CuO NPs and CMC-CuO NPs increases from 42.11% to 85.16% when increasing time in the prior 30–180 min. When the contact time exceeded 180 min, the TC removal efficiency decreased insignificantly. The data clearly show that the removal percent of TC by CMC-dispersed CuO nanoparticles (0.5CMC-CuO NPs (76.12%), 1.0CMC-CuO NPs (81.20%), 1.5CMC-CuO NPs (84.73%), and 2.0CMC-CuO NPs (85.16%)) was considerably higher than that of CuO NPs (63.93%) at 180 min so that 180 min is the best contact time for TC removal.

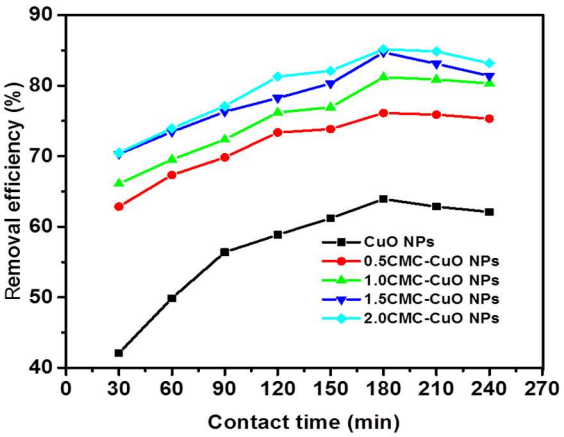

Figure 7. Effect of contact time on the TC removal using CuO NPs and CMC-CuO NPs (C_i = 10 mg/L, pH 5).

3.2.4 Effect of adsorbent dosage

The effect of adsorbent dosage on TC removal using CuO NPs and CMC-CuO NPs was investigated in the range of 0.1–0.5 g at 180 min and is indicated in **Figure 8**. As can be seen in **Figure 8**, the TC removal increased when the adsorbent dosage increased from 0.1 to 0.5 g as the result of rising the net surface charge or specific surface area of the adsorbent. The TC plateau removal efficiency was achieved at 0.3 g as 63.14% (CuO NPs), 79.2% (0.5CMC-CuO NPs), 80.23% (1.0CMC-CuO NPs), 84.13% (1.5CMC-CuO NPs), 86.97% (2.0CMC-CuO NPs), and was not changed significantly when the amount of adsorbent was above 0.3 g. Therefore, we used 0.3 g dosage for further study on TC removal.

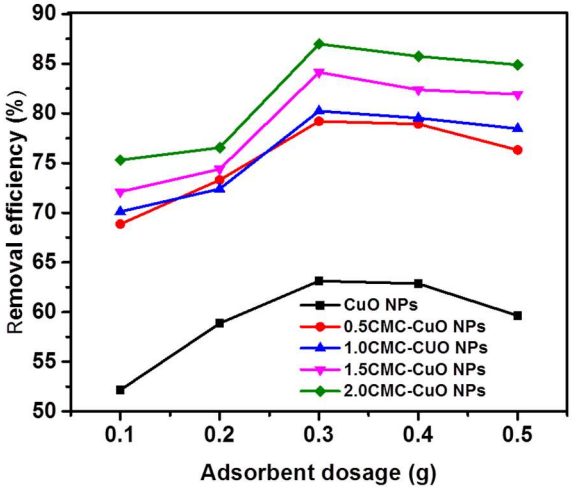

Figure 8. Effect of adsorbent dosage on the TC removal using CuO NPs and CMC-CuO NPs (C_i = 10 mg/L, pH 5, 180 min).

4. Conclusion

In this research, the pure CuO NPs and CMC-CuO nanoparticles were successfully prepared by the co-precipitation method and applied for the removal of tetracycline from an aqueous model solution. The prepared CuO NPs and CMC-CuO nanoparticles were characterized by XRD, FTIR, SEM and TG-DTA techniques. The CMC-CuO NPs were completely consistent with the diffraction peaks of CuO NPs. X-ray diffraction (XRD) studies confirmed the formation of CuO nanoparticles in the CMC matrix with an average crystallite range of 38.16–61.28 nm with the CMC matrix. FTIR spectra showed that CMC attached

CuO NPs were formed successfully after the chemical effect of CMC on CuO NPs. The SEM image of CuO NPs revealed the aggregated morphology. The SEM images of all CMC-CuO NPs show a cluster due to agglomeration. In TGDTA thermograms, it was found that the total weight loss of CMC-CuO NPs is higher than that of pure CuO NPs. However, the FTIR and TG-DTA data indicate that the functional groups were successfully attached to the surface of the nanoparticles. The sorption capacities of prepared samples were studied for the removal of tetracycline from aqueous model solutions with varying experimental conditions of the initial concentration, pH, contact time, and dosage. It is found that the removal percent of tetracycline increases with not only a decrease in initial concentration, but also an increase in contact time and amount of dosage. These carboxymethyl cellulose/CuO nanoparticles may be intended to have a good potential, effective nanoadsorbents for rapid removal of tetracycline which are a problem of clinical wastewater and other sources of the water system. On account of the outcomes, we do advise that carboxymethyl cellulose/CuO nanoparticles can also be used to remove tetracycline in an aqueous solution. It is recommended that the researchers of polymer-based nanomaterials be kept informed of this study. Future researchers are encouraged to investigate other factors that may affect the performance of carboxymethylcellulose/CuO nanoparticles.

Acknowledgments

The authors fully acknowledged the Ministry of Education (MOE), Department of Higher Education and Department of Chemistry, University of Yangon for the approved support which makes this important research.

Author contributions

Conceptualization, WPPP and YT; methodology, WPPP; software, ATH; validation, WPPP, MTK and NS; formal analysis, WPPP; investigation, WPPP; resources, WPPP; data curation, WPPP; writing—original draft preparation, YT, MTK, NS and ATH; writing—review and editing, YT and MTK; visualization, NS; supervision, ATH; project administration, ATH; funding acquisition, ATH. All authors have read and agreed to the published version of the manuscript.

Conflict of interest

The authors declare no conflict of interest.

References

1. Alothman ZA, Badjah AY, Alharbi OML, *et al*. Copper carboxymethyl cellulose nanoparticles for efficient removal of tetracycline antibiotics in water. Environmental Science and Pollution Research 2020; 27: 42960–42968. doi: 10.1007/s11356-020-10189-1.
2. Min H, Kan JE. Engineered biochar from agricultural waste for removal of tetracycline in water. Bioresource Technology 2019; 284: 437–447. doi: 10.1016/j.biortech.2019.03.131.
3. Nguyen VT, Nguyen TB, Chen CW, *et al*. Cobalt-impregnated biochar (Co-SCG) for heterogeneous activation of peroxymonosulfate for removal of tetracycline in water. Bioresource Technology 2019; 292: 121954. doi: 10.1016/j.biortech.2019.121954.
4. Rizzi V, Lacalamita D, Gubitosa J, *et al.* Removal of tetracycline from polluted water by chitosan-olive pomace adsorbing films. Science of The Total Environment 2019; 693: 133620. doi: 10.1016/j.scitotenv.2019.133620.
5. Sun H, Shi X, Mao J, *et al*. Tetracycline sorption to coil and soil of humic acid: An examination of humic structural heterogeneity. Environmental Toxicology and Chemistry 2010; 29(9): 1934–1942. doi: 10.1002/etc.248.
6. Vu TH, Ngo TMV, Duong TTA, *et al*. Removal of tetracycline from aqueous solution using nanocomposite based on polyanion-modified laterite material. Journal of Analytical Methods in Chemistry 2020; 2020: 6623511. doi: 10.1155/2020/6623511.
7. Hattori K, Abe E, Yoshida T, *et al*. New solvents for cellulose. II. ethylenediamine/thiocyanate salt system. Polymer Journal 2004; 36: 123–130. doi: 10.1295/polymj.36.123.
8. Rachtanapun P. Blended films of carboxymethyl cellulose from papaya peel (CMCp) and corn starch. Kasetsart Journal–Natural Science 2009; 43(5): 259–266.
9. Tijsen CJ, Kolk HJ, Stamhuis EJ, *et al*. An experimental study on the carboxymethylation of granular potato starch in non-aqueous media. Carbohydrate Polymers 2001; 45(3): 219–226. doi: 10.1016/S0144-8617(00)00243-5.
10. Singh RK, Singh AK. Optimization of reaction conditions for preparing carboxymethyl cellulose from corn cobic agricultural waste. Waste and Biomass Valorization 2013; 4: 129–137. doi: 10.1007/s12649-012-9123-9.

11. Bono A, Ying PH, Yan FY, *et al*. Synthesis and characterization of carboxymethyl cellulose from palm kernel cake. Advances in Natural and Applied Sciences 2009; 3(1): 5–11.
12. Youssef AM, Assem FM, El-Sayed HS, *et al*. Synthesis and evaluation of eco-friendly carboxymethyl cellulose/polyvinyl alcohol/CuO bionanocomposites and their use in coating processed cheese. RSC Advances 2020; 10: 37857–37870. doi: 10.1039/D0RA07898K.
13. Awwad AM, Albiss BA, Salem NM. Antibacterial activity of synthesized copper oxide nanoparticles using Malva sylvestris leaf extract. SMU Medical Journal 2015; 2(1): 91–101.
14. Yadollahi M, Gholamali I, Namazi H, *et al*. Synthesis and characterization of antibacterial carboxymethylcellulose/CuO bio-nanocomposite hydrogels. International Journal of Biological Macromolecules 2015; 73: 109–114. doi: 10.1016/j.ijbiomac.2014.10.063.
15. Basta AH, Lotfy VF, Eldewany C. Comparison of copper-crosslinked carboxymethyl cellulose versus biopolymer-based hydrogels for controlled release of fertilizer. Polymer-Plastics Technology and Materials 2021; 60(17): 1884–1897. doi: 10.1080/25740881.2021.1934017.
16. Chen W-R, Huang C-H. Adsorption and transformation of tetracycline antibiotics with aluminum oxide. Chemosphere 2010; 79(8): 779–785. doi: 10.1016/j.chemosphere.2010.03.020.
17. Parolo ME, Savini MC, Vallés JM, *et al*. Tetracycline adsorption on montmorillonite: pH and ionic strength effects. Applied Clay Science 2008; 40(1–4): 179–186. doi: 10.1016/j.clay.2007.08.003.